Chapter 14

The input parameter

14.1 The nucleus - properties and composition

The radius of the model nucleus was set to 25 km Altenhoff *et al.* [1999].
In order to run the ComChem model the initial abundances within the coma have to be defined for each heliocentric distance used. The ComChem model as used in this study does not include a sublimation model. For this reason the values for surface albedo and emissivity are not relevant. They are included only for completeness and are set to an albedo of 4% and an emissivity of 96% (see for example Keller *et al.* [1986]). The modeling itself does not start on the nucleus surface, but in a shell approximately 1 m above the surface. Therefore instead of nucleus abundances the composition in the coma is given. Details are discussed in section 12.3.
The composition used for this study consists of 22 species. For all these species abundances for comet Hale-Bopp are given in Bockelée-Morvan *et al.* [2000]. The species are listed in table 14.1. Each column represents the production rates used for the heliocentric distance denoted at the top of the column. The bottom row gives the assumed surface temperature (see below). For species labeled with (1) the production rates of Biver *et al.* [1997] have been used. The values have been interpolated, or if necessary extrapolated, to the heliocentric distance of the observation. The extrapolation assumed a $Q \sim r_h^b$ relationship with b constant over the whole range of heliocentric distances covered in this study. Figure 14.1 shows as an example the measured production rates of CO by Biver *et al.* [1997] and the values assumed for the model setups.
There are only very few measurements for the water production rates available for heliocentric distances greater than 3 AU. From this distance outward a severe decrease in the water sublimation is expected (see chapter 4). Therefore the assumption of $Q(H_2O) \sim r_h^b$ with a constant b as used above is not valid for the extrapolation of water production rates to larger heliocentric distances. For this work a water sublimation model by Huebner and Benkhoff [1999] and Benkhoff and Huebner [1995] was used and adjusted using the available measurements of $Q(H_2O)$. The model assumes a porous nucleus with water ice as the major component and a number of minor ice components with higher volatility. It assumes a Hale-Bopp like orbit and orientation of the spin-axis. As can be seen in figure 14.2 this

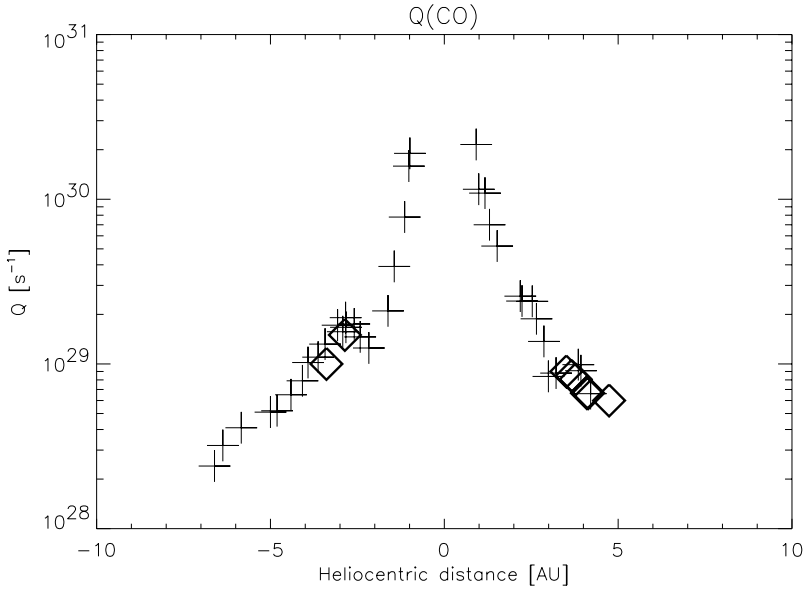

Figure 14.1: CO production rate (diamonds) estimated for the modeling and CO rates (crosses) measured by Biver *et al.* [1997]

model is in good agreement with the values by Weaver *et al.* [1999b] and Dello Russo *et al.* [2000] for the post-perihelion measurements. Comet Hale-Bopp showed a slightly higher water production pre-perihelion. However, the differences between the estimated and the measured production rates are less than a factor of 2. It will be shown later, that this has no significant effect on the results. The same model yields from the energy balance at the surface the surface temperature T_0 which is shown in the bottom row of table 14.1. This value has little influence on the modeling, since the temperature of the bulk gas is calculated within the model in a self-consistent way (see section 12.1).
The production rates for CO_2 have been extrapolated based on the values obtained by Weaver *et al.* [1999b], assuming that the activity scales with heliocentric distance like CO.
For CS_2 (labeled with (3) in table 14.1) the production rate of CS was used, assuming that there is no other significant source of CS. A comparison with the measurements for $Q(CS_2)$ by Weaver *et al.* [1999b] shows very good agreement.
For species (labeled with a (2) in table 14.1) which have not been observed at large heliocentric distance the production rates had to be estimated. For these species it was assumed, that the abundance ratio relative to Q(HCN) was constant. As was shown in 10 it was shown that HCN is the dominant parent of CN. Using this result the production rate for the unknown species can then be estimated using Q(CN). The abundance ratios near perihelion were obtained from Bockelée-Morvan *et al.* [2000].
Most of these species have a very low abundance and all of the species play a negligible role in the chemistry for the formation of C_2 and C_3. Even a larger error in the estimates of their production rates has no significant effect on the results. This has been shown in a sensitivity analysis (see section 19).

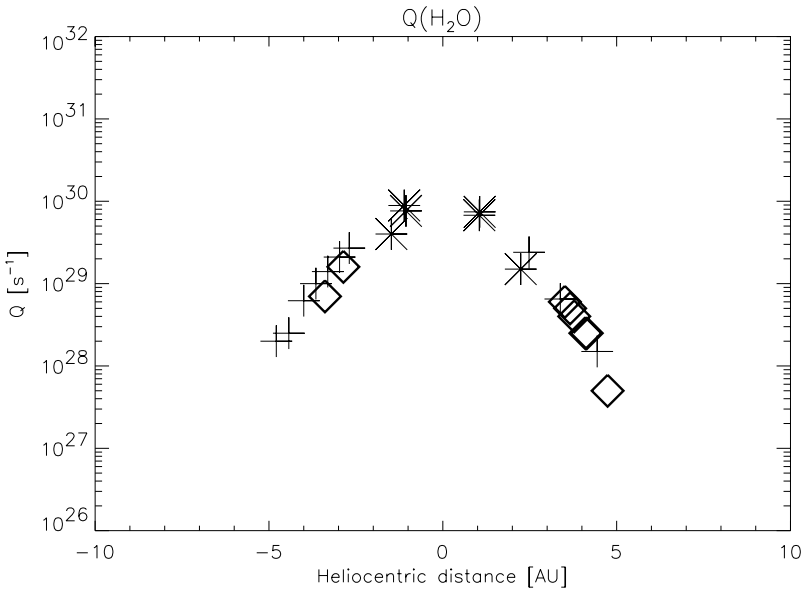

Figure 14.2: Water production rate (diamonds) estimated for the model input and water production rates (crosses) measured by Weaver *et al.* [1999b] and (stars) Dello Russo *et al.* [2000]

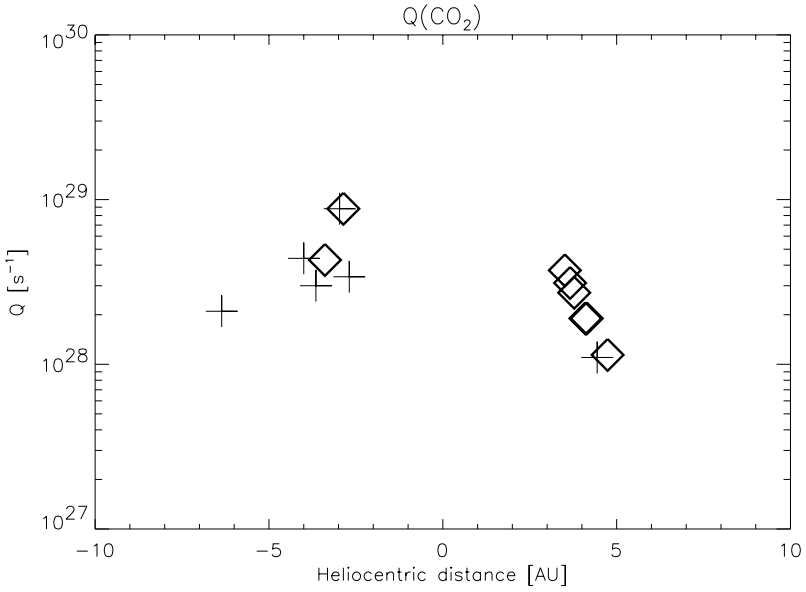

Figure 14.3: Carbon dioxide production rates (diamonds) estimated for the modeling and production rates (crosses) measured by Weaver *et al.* [1999b]

To allow an easy comparison of different sets of production rates for the different heliocentric distances, the production rates are transformed in a relative abundance $A_{species}$ for each

r_h [AU]	3.51	3.66	3.78	4.1	4.14	4.74	-2.86	-3.39
	Production rate [10^{25} molecule s^{-1}]							
H_2O	6000.	5000.	4000.	2500.	2500.	500.	16000.	7000.
CO_2	3720.	3117.	2720.	1900.	1900.	1140.	8800.	4300.
CO (1)	9000.	8462.	8070.	6652.	6652.	6000.	15000.	10000.
CH_3OH (1)	500.0	473.8	454.5	352.5	352.5	160.0	1000.	530.
H_2CO (1)	40.00	35.17	31.86	21.56	21.56	12.80	75.0	43.0
H_2CS (2)	4.152	3.940	3.789	2.935	2.935	1.329	5.4	4.0
CH_4 (2)	124.9	118.4	113.6	88.05	88.05	39.86	160.0	131.0
NH_3 (2)	14.58	13.82	13.26	10.27	10.27	4.666	19.0	15.0
HCN (1)	40.00	35.69	32.68	24.82	24.82	20.00	76.0	45.0
HNC (1)	1.002	0.910	0.844	0.570	0.570	0.320	2.8	1.4
N_2 (2)	50.40	42.65	37.50	16.71	16.71	16.13	120.0	57.0
H_2S (1)	350.0	327.3	310.9	220.1	220.1	112.0	640.0	365.0
CS_2 (3)	12.16	10.37	9.168	6.485	6.485	3.201	27.0	14.0
OCS (2)	83.32	78.96	75.75	58.70	58.70	26.67	110.0	87.0
SO (2)	60.40	57.24	54.92	42.56	42.56	19.33	80.0	63.0
SO_2(2)	47.91	45.40	43.56	33.75	33.75	15.33	63.0	50.0
CH_3CN (1)	4.500	4.140	3.880	2.935	2.935	1.440	8.50	5.1
NH_2CH_3 (2)	402.0	339.6	298.1	212.6	212.6	128.6	920.0	460.
HCOOH (2)	22.91	19.39	17.04	13.21	13.21	7.33	52.0	26.0
T_0 [K]	182.	181.	181.	180.	180.	173.	185	182

Table 14.1: The composition and surface temperature assumed as input parameter for the ComChem model for each of the 8 heliocentric distances used in this study. The upper indexes denote the method used to derive the production rates. (1) Production rates interpolated from Biver *et al.* [1997], (2) species not observed at large heliocentric distances, values are extrapolations (3) production rate of CS was assumed

species and the total surface activity Z.
The relative abundances are normalized to water. The surface activity is then given by

$$Z = \frac{Q(\mathrm{H_2O})}{4 \cdot \pi r_n^2} \cdot \frac{A_{\mathrm{total}}}{A_{\mathrm{Water}}} \tag{14.1}$$

$Q(\mathrm{H_2O})$	water production rate
r_n	Radius of the nucleus
A_{water}	relative abundance of water
A_{total}	sum of the relative abundance of all species

Changing the production rate of one species results in a change of its relative abundance A_{Species} and in the surface activity Z. The production rates of all other species remain

unchanged. Increasing the C_2H_6 production rate $Q(C_2H_6)$ for example will increase its relative abundance $A(C_2H_6)$ compared to water and will increase the overall activity of the comet. The conversion from a relative abundance to the production rate is done by

$$Q_{\text{Species}} = \frac{A_{\text{Species}}}{A_{\text{total}}} \cdot Z \cdot 4 \cdot \pi r_n^2 \tag{14.2}$$

14.2 The model coma chemistry input parameters

The reaction network for the coma chemistry has to be defined. While the whole reaction network consists of more than 1000 reactions only a subset of these play a significant role in the formation of the C_2 and C_3 radical. Approximately 200 reactions are related to the chemistry discussed here. Out of these reaction approximately 20 dominate the formation of C_2 or C_3. The reaction rates for the latter ones are discussed in this section, while a complete list of the related reactions is given in appendix E.
Two types of reactions clearly dominate for heliocentric distances larger than 3AU. These are photodissociation and dissociation by electron impact.

14.2.1 Photodissociation reactions

The chemistry for the formation of the C_2 radical has been described in section 11.1. The photodissociation rate coefficients have been obtained mainly from Huebner *et al.* [1992]. The values are in good agreement with recent data by Moses [2000]. For C_2H_2 Wu [2000] has provided recent unpublished laboratory measurements of absorption cross sections at low temperatures. A comparison of the resulting dissociation rate coefficients showed difference of less than a factor of two compared to the values obtained by Moses [2000] and Huebner *et al.* [1992]. For this work the values by Huebner *et al.* [1992] have been used for the C_2H_2 photodissociation. Once the complete measurements by Wu [2000] are available these values can be updated.
The C_3 chemistry has been described in detail in section 11.2. Moses [2000] provided rate coefficients for most of the reactions (see table 14.3). The coefficients have originally been calculated for the atmospheric chemistry of Jupiter and Saturn (see also Gladstone *et al.* [1996]). The rates used in this work have been recalculated by Moses for the condition of near vacuum and a heliocentric distance of 1 AU. The reaction rates for C_3H_4 reflect a mixture of 50% allene and 50% propyne.

14.2.2 Deriving C_3H_2 and C_3 photodissociation rates

As has been discussed in section 11.2 the reaction rate for the dissociation of C_3H_2

$$R_1 : C_3H_2 + h\nu \longrightarrow C_3 + H_2$$

is basically unknown and the reaction rate for the photodissociation of C_3

$$R_2 : C_3 + h\nu \longrightarrow C_2 + C$$

is only based on estimates see for example Huebner *et al.* [1992].
However, the measurements of radial profiles of the C_3 radical at a number of heliocentric distances allow to derive a good estimate for the two missing reaction rates. The estimates have been derived by running the ComChem model with different combinations of reaction rates for reactions R_1 and R_2. For each combination of reaction rates the best match between modeled and measured C_3 profile was derived. For details on the fitting procedure see step 2 in section 15. The quality of the match is determined by the χ^2 error of the fit. Figures 14.4 and 14.5 show the range of reaction rates scanned for reactions R_1 and R_2 and as a colored contour plot the χ^2 values. The global minimum in the χ^2 values marks the best fitting pair of reaction rates. It is determined using a bi-linear minimization routine [Press *et al.*, 1992]. The position of the minimum, which is equivalent to a pair of reaction rates for reaction R_1 and R_2 is listed in table 14.2 for each night.

Date	R_1 [10^{-7} s^{-1}]	R_2 [10^{-7} s^{-1}]
23.11.1997	9.5±2.4	195.±15.
6.12.1997	15.4±5.1	202.±22.
19.12.1997	9.4±0.5	200.±12.
20.1.1998	9.6±3.2	202.±20.
21.1.1998	9.6±6.1	199.±13.4
21.3.1998	9.4±3.1	188.±20.0
17.8.1996	15.6±4.1	143.±45.0
2.10.1996	8.9±3.2	201.±15.0

Table 14.2: Derived reaction rates for reactions R_1 and R_2 normalized to r_h=1AU

The results for the photodissociation of C_3H_2 agree within the errors over all observed nights. Two nights observed at the Danish 1.54m telescope (6.12.1997 and 17.8.1996) show a deviation to higher values. This is most likely caused by the contamination of the C_3 profile. Therefore to determine a mean value for the reaction rate these two nights have been excluded. The derived mean is R_1=9.5± 0.3 $\cdot 10^{-7}$ s^{-1}.
The results for the photodissociation of C_3 agree within the errors over all observed nights. Only the value obtained for the night 17.8.1996 shows a slight deviation, but for consistency with the calculations for R_1 the night 6.12.1997 was excluded as well. Since this data was obtained at the Danish 1.54m telescope the deviation is presumably caused by the contamination of the C_3 profile. Taking the mean value of the remaining nights yields a reaction rate coefficient of r_2=200.± 5.5 $\cdot 10^{-7}$ s^{-1}.

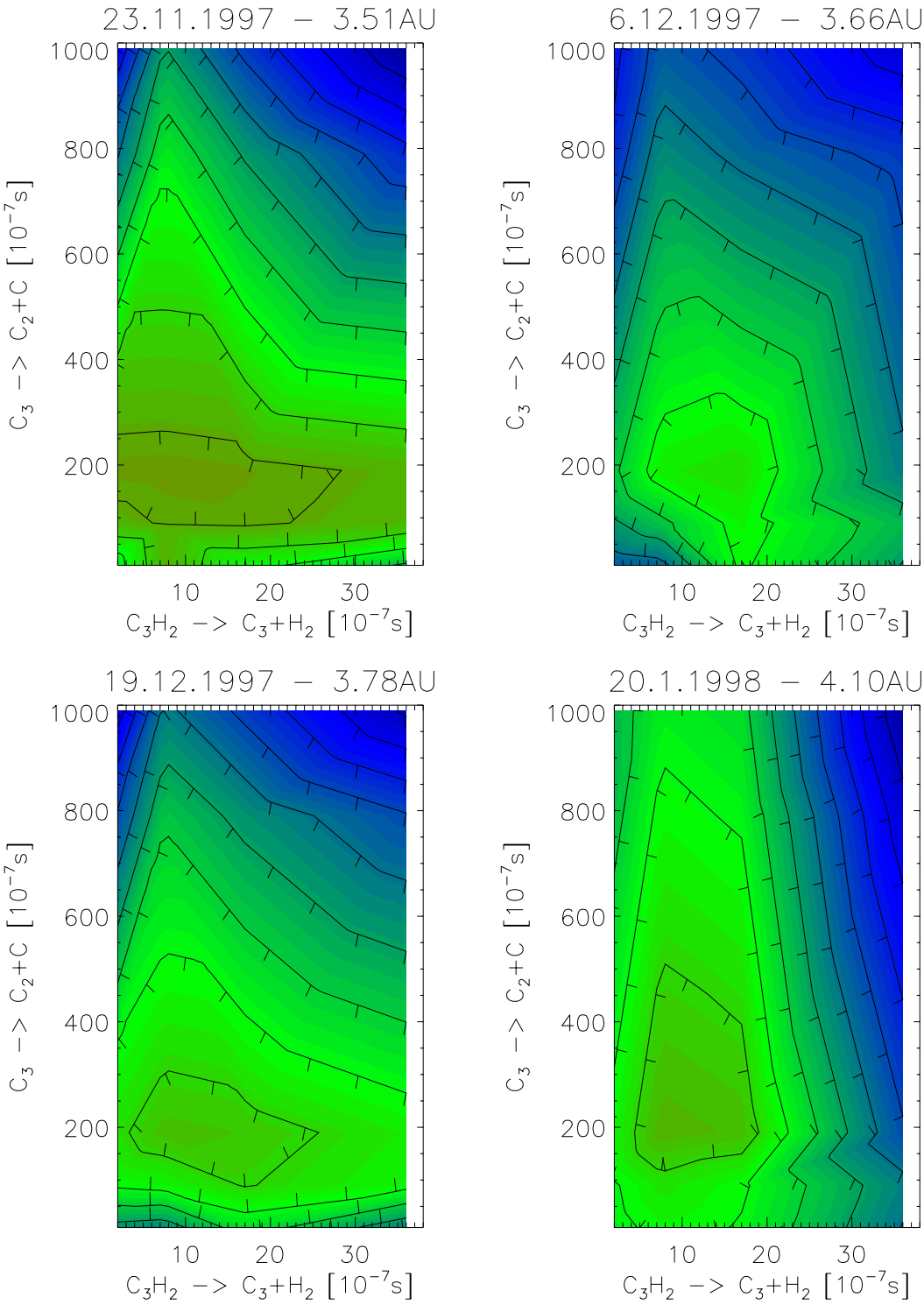

Figure 14.4: Colored contour plot of the χ^2 values vs. the reactions rates for reactions R_1 and R_2

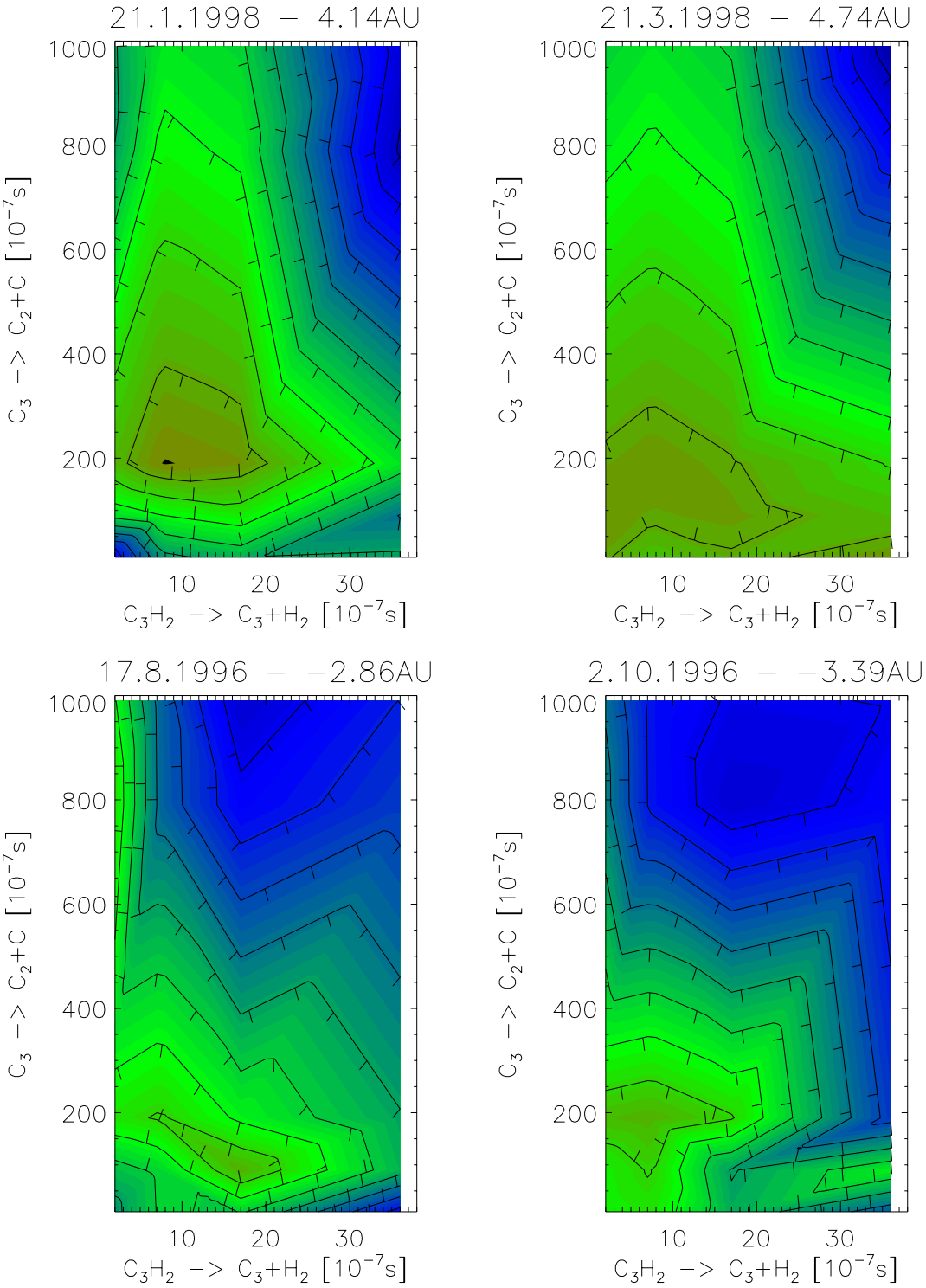

Figure 14.5: Colored contour plot of the χ^2 values vs. the reactions rates for reactions R_1 and R_2 (cont.)

14.2.3 Electron impact dissociation reactions

As has been discussed in sections 11.1 and 11.2 there is very little laboratory work done on cross sections for electron impact dissociation of hydrocarbons. Most of the reaction rates used in this work are based on theoretical work by Keady and Huebner (published in Schmidt *et al.* [1988] and Boice *et al.* [1986]). As discussed in section 11.1 only recently new work has been started by the Plasma-Material Interaction Group at the University of Illinois, Urbana-Champaign [Alman and Ruzic, 2000]. However the uncertainties in these newly determined values are even larger than in the theoretically determined values. For this study the values by Keady and Huebner have been adopted (see Table 14.3). The sensitivity studies in section 19.2.3 will show that even an uncertainty of one magnitude in the estimate for the reaction rate coefficients has very little effect on the resulting profiles.

Reactants				Products					Rate coefficent [s^{-1}]	Reference
C_2H_6	+	$h\nu$	$\longrightarrow$	C_2H_5	+	H			$3.28{\cdot}10^{-6}$	[Huebner *et al.*, 1992]
C_2H_6	+	$h\nu$	$\longrightarrow$	C_2H_4	+	H_2			$3.67{\cdot}10^{-6}$	[Huebner *et al.*, 1992]
C_2H_6	+	$h\nu$	$\longrightarrow$	CH_3	+	CH_3			$8.80{\cdot}10^{-7}$	[Huebner *et al.*, 1992]
C_2H_6	+	$h\nu$	$\longrightarrow$	CH_2	+	CH_4			$2.22{\cdot}10^{-6}$	[Huebner *et al.*, 1992]
C_2H_5	+	$h\nu$	$\longrightarrow$	C_2H_2	+	H_2	+	H	$1.00{\cdot}10^{-6}$	[Boice, 2000]
C_2H_4	+	$h\nu$	$\longrightarrow$	C_2H_2	+	H_2			$2.40{\cdot}10^{-5}$	[Huebner *et al.*, 1992]
C_2H_4	+	$h\nu$	$\longrightarrow$	C_2H_2	+	H	+	H	$2.30{\cdot}10^{-5}$	[Huebner *et al.*, 1992]
C_2H_4	+	$h\nu$	$\longrightarrow$	CH_2	+	CH_2			$6.00{\cdot}10^{-5}$	[Huebner *et al.*, 1992]
C_2H_2	+	$h\nu$	$\longrightarrow$	C_2	+	H_2			$2.74{\cdot}10^{-6}$	[Huebner *et al.*, 1992]
C_2H_2	+	e	$\longrightarrow$	C_2	+	H_2	+	e	$1.90{\cdot}10^{-8}$	[Schmidt *et al.*, 1988]
C_2H_2	+	$h\nu$	$\longrightarrow$	C_2H	+	H			$1.02{\cdot}10^{-5}$	[Huebner *et al.*, 1992]
C_2H_2	+	e	$\longrightarrow$	C_2H	+	H	+	e	$1.90{\cdot}10^{-8}$	[Schmidt *et al.*, 1988]
C_2H	+	$h\nu$	$\longrightarrow$	C_2	+	H			$3.00{\cdot}10^{-5}$	[Huebner *et al.*, 1992]
C_2	+	$h\nu$	$\longrightarrow$	C	+	C			$1.40{\cdot}10^{-7}$	[Huebner *et al.*, 1992]
C_2	+	$h\nu$	$\longrightarrow$	C_2^+	+	e			$9.10{\cdot}10^{-7}$	[Huebner *et al.*, 1992]
C_2	+	e	$\longrightarrow$	C	+	C	+	e	$9.43{\cdot}10^{-10}$	[Schmidt *et al.*, 1988]
C_3H_4	+	$h\nu$	$\longrightarrow$	C_3H_3	+	H			$1.33{\cdot}10^{-4}$	[Moses, 2000]
C_3H_4	+	$h\nu$	$\longrightarrow$	C_3H_2	+	H_2			$2.96{\cdot}10^{-5}$	[Moses, 2000]
C_3H_4	+	e	$\longrightarrow$	C_3	+	H_2	+	H_2 + e	$3.80{\cdot}10^{-8}$	[Schmidt *et al.*, 1988]
C_3H_3	+	$h\nu$	$\longrightarrow$	C_3H_2	+	H			$1.82{\cdot}10^{-3}$	[Moses, 2000]
C_3H_2	+	$h\nu$	$\longrightarrow$	C_3	+	H_2			$\mathbf{9.50}{\cdot}10^{-7}$	Helbert [this work]
* C_3H_2	+	$h\nu$	$\longrightarrow$	C_3	+	H_2			$\mathit{1.9}{\cdot}10^{-6}$	[Moses, 2000]
C_3	+	$h\nu$	$\longrightarrow$	C_2	+	C			$\mathbf{2.00}{\cdot}10^{-5}$	Helbert [this work]
* C_3	+	$h\nu$	$\longrightarrow$	C_2	+	C			$\mathit{1.00}{\cdot}10^{-4}$	[Huebner *et al.*, 1992]
CH_4	+	$h\nu$	$\longrightarrow$	CH_3	+	H			$2.64{\cdot}10^{-7}$	[Huebner *et al.*, 1992]
CH_4	+	e	$\longrightarrow$	CH_3	+	H	+	e	$9.43{\cdot}10^{-10}$	[Schmidt *et al.*, 1988]
CH_4	+	$h\nu$	$\longrightarrow$	CH_2	+	H_2			$5.44{\cdot}10^{-6}$	[Huebner *et al.*, 1992]
CH_4	+	$h\nu$	$\longrightarrow$	CH_2	+	H	+	H	$2.14{\cdot}10^{-6}$	[Huebner *et al.*, 1992]
CH_4	+	$h\nu$	$\longrightarrow$	CH	+	H_2	+	H	$6.39{\cdot}10^{-7}$	[Huebner *et al.*, 1992]
CH_2	+	$h\nu$	$\longrightarrow$	CH	+	H			$2.00{\cdot}10^{-5}$	[Huebner *et al.*, 1992]
CH	+	$h\nu$	$\longrightarrow$	C	+	H			$4.16{\cdot}10^{-3}$	[Huebner *et al.*, 1992]
CH_3CN	+	$h\nu$	$\longrightarrow$	CH_3	+	CN			$5.00{\cdot}10^{-5}$	[Huebner *et al.*, 1992]
CH_3CN	+	e	$\longrightarrow$	CH_3	+	CN	+	e	$3.80{\cdot}10^{-8}$	[Huebner *et al.*, 1992]

Table 14.3: The main reactions and their reaction rates. The asterisks mark reactions for which rate coefficients have been derived in this work. Coefficients which have been derived in this work are printed in bold, while the old estimates for these coefficients are printed in italics. A complete list of reactions related to the C_2 and C_3 chemistry is given in appendix E.